Arabidopsis plasma membrane protein crucial for Ca^{2+} influx and touch sensing in roots

Yuko Nakagawa[a,b,c,d], Takeshi Katagiri[c], Kazuo Shinozaki[b,c], Zhi Qi[e,f], Hitoshi Tatsumi[b,e], Takuya Furuichi[e], Akio Kishigami[b,e], Masahiro Sokabe[e,g,h], Itaru Kojima[d], Shusei Sato[i], Tomohiko Kato[i,j], Satoshi Tabata[i], Kazuko Iida[k], Asuka Terashima[a,b,l], Masataka Nakano[a,b], Mitsunobu Ikeda[a,b,m], Takuya Yamanaka[a,b], and Hidetoshi Iida[a,b,n]

[a]Department of Biology, Tokyo Gakugei University, Tokyo 184-8501, Japan; [b]Core Research for Evolutional Science and Technology (CREST) and [h]ICORP Cell Mechanosensing, Japan Science and Technology Agency, Saitama 332-0012, Japan; [c]Laboratory of Plant Molecular Biology, RIKEN Tsukuba Institute, Ibaraki 305-0074, Japan; [d]Laboratory of Cell Physiology, Institute for Molecular and Cellular Regulation, Gunma University, Gunma 371-8510, Japan; [e]Department of Physiology, Nagoya University Graduate School of Medicine, Aichi 466-8550, Japan; [f]State Key Laboratory of Brain and Cognitive Science, Institute of Biophysics, Beijing 100101, People's Republic of China; [g]Department of Molecular Physiology, National Institute for Physiological Sciences, Aichi 444-8585, Japan; [i]Laboratory of Plant Gene Research, Kazusa DNA Research Institute, Chiba 292-0818, Japan; and [k]Biomembrane Signaling Project 2, Tokyo Metropolitan Institute of Medical Science, Tokyo 113-8613, Japan

Edited by Daniel J. Cosgrove, Pennsylvania State University, University Park, PA, and approved December 20, 2006 (received for review September 3, 2006)

Plants can sense and respond to mechanical stimuli, like animals. An early mechanism of mechanosensing and response is speculated to be governed by as-yet-unidentified sensory complexes containing a Ca^{2+}-permeable, stretch-activated (SA) channel. However, the components or regulators of such complexes are poorly understood at the molecular level in plants. Here, we report the molecular identification of a plasma membrane protein (designated Mca1) that correlates Ca^{2+} influx with mechanosensing in *Arabidopsis thaliana*. *MCA1* cDNA was cloned by the functional complementation of lethality of a yeast *mid1* mutant lacking a putative Ca^{2+}-permeable SA channel component. Mca1 was localized to the yeast plasma membrane as an integral membrane protein and mediated Ca^{2+} influx. Mca1 also increased $[Ca^{2+}]_{cyt}$ upon plasma membrane distortion in *Arabidopsis*. The growth of *MCA1*-overexpressing plants was impaired in a high-calcium but not a low-calcium medium. The primary roots of *mca1*-null plants failed to penetrate a harder agar medium from a softer one. These observations demonstrate that Mca1 plays a crucial role in a Ca^{2+}-permeable SA channel system that leads to mechanosensing in *Arabidopsis*. We anticipate our findings to be a starting point for a deeper understanding of the molecular mechanisms of mechanotransduction in plants.

calcium | calcium channel | calcium uptake | mechanosensing

Sensing and responding to mechanical stimuli, such as touch, gravity, flexure, and turgor, are fundamental characteristics of plants (1–3). Because the mechanical stimulation of plants immediately elicits a transient rise in the cytosolic Ca^{2+} concentration, $[Ca^{2+}]_{cyt}$, an early mechanism of mechanosensing and response is thought to be governed by mechanical sensors with a Ca^{2+}-permeable, stretch-activated (SA) channel as an essential constituent (4–6). Thus, the SA channel is postulated to play a major role in the regulation of thigmotropism, gravitropism, the morphogenesis of organs including roots, and polarized growth of pollen tubes (7–9). However, the molecular identities of the channel and its regulators are unknown and their physiological functions are speculative, except for MscS-like proteins located in the plastid envelope in *Arabidopsis thaliana* (10).

The yeast *Saccharomyces cerevisiae* is a helpful eukaryote in isolating and characterizing plant membrane proteins. K^+ channel cDNAs of *Arabidopsis* have been cloned by complementation of K^+ uptake-deficient mutants of *S. cerevisiae* with *Arabidopsis* cDNA libraries (11, 12). Putative cyclic nucleotide-gated cation channels, found in the *Arabidopsis* genome, are successfully expressed in *S. cerevisiae* mutants defective in K^+ uptake or Ca^{2+} uptake and their function and subcellular localization have been characterized (13, 14).

Here, we report the isolation and characterization of an *Arabidopsis* cDNA (designated *MCA1*) that complements the lethal phenotype of an *S. cerevisiae mid1* mutant defective in a putative Ca^{2+}-permeable SA channel component. We demonstrate that Mca1 is an integral plasma membrane protein that mediates Ca^{2+} uptake when expressed in *S. cerevisiae*. *MCA1* mRNA is detected at varying levels in all *Arabidopsis* tissues examined, as revealed by Northern blotting. With the analyses of *Arabidopsis* mutants lacking or overexpressing *MCA1*, we suggest that Mca1 is an important constituent of a mechano-stimulated Ca^{2+} uptake mechanism in *Arabidopsis*.

Results

Isolation and Characterization of *MCA1* cDNA. To isolate a candidate gene encoding a component or regulator of a Ca^{2+}-permeable SA channel from *Arabidopsis*, we used functional complementation of the lethal phenotype of the *mid1* mutant of the yeast *S. cerevisiae*, which lacks a putative Ca^{2+}-permeable SA channel component and becomes lethal because of a deficiency of Ca^{2+} influx during exposure to mating pheromone (15–17). The *mid1* mutant was transformed with an *Arabidopsis* cDNA library constructed in a yeast expression vector (18). The transformants were screened for their viability after being exposed to mating pheromone. One viable transformant was obtained, and the full-length cDNA on the plasmid isolated from it was designated *MCA1* for *mid1*-complementing activity 1. Quantitative assays showed that *MCA1* indeed partially complemented the lethality of *mid1* cells (Fig. 1*A*) and increased Ca^{2+} uptake activity (Fig. 1*B*). It should be noted that *MCA1*-expressing *mid1* cells grew slightly slower than *mid1* and wild-type cells. Therefore, the higher Ca^{2+} uptake in the *MCA1*-expressing *mid1* cells is not due to their putative, higher growth rate.

Nucleotide sequencing of the *MCA1* cDNA identified the corresponding hypothetical ORF At4g35920 on chromosome 4.

Author contributions: K.S., M.S., I.K., S.T., and H.I. designed research; Y.N., T. Katagiri, Z.Q., H.T., T.F., A.K., S.S., T. Kato, K.I., A.T., M.N., M.I., and T.Y. performed research; and H.I. wrote the paper.

The authors declare no conflict of interest.

This article is a PNAS direct submission.

Freely available online through the PNAS open access option.

Abbreviations: SA, stretch activated; TNP, trinitrophenol.

[j]Present address: Forestry Research Institute, Oji Paper Co., Ltd., Mie 519-0212, Japan.

[l]Present address: Laboratory for Immune Regulation, RIKEN Research Center for Allergy and Immunology, Yokohama 230-0045, Japan.

[m]Present address: Department of Medical Biochemistry, Graduate School of Medicine, Tokyo Medical and Dental University, Tokyo 113-8519, Japan.

[n]To whom correspondence should be addressed. E-mail: iida@u-gakugei.ac.jp.

This article contains supporting information online at www.pnas.org/cgi/content/full/0607703104/DC1.

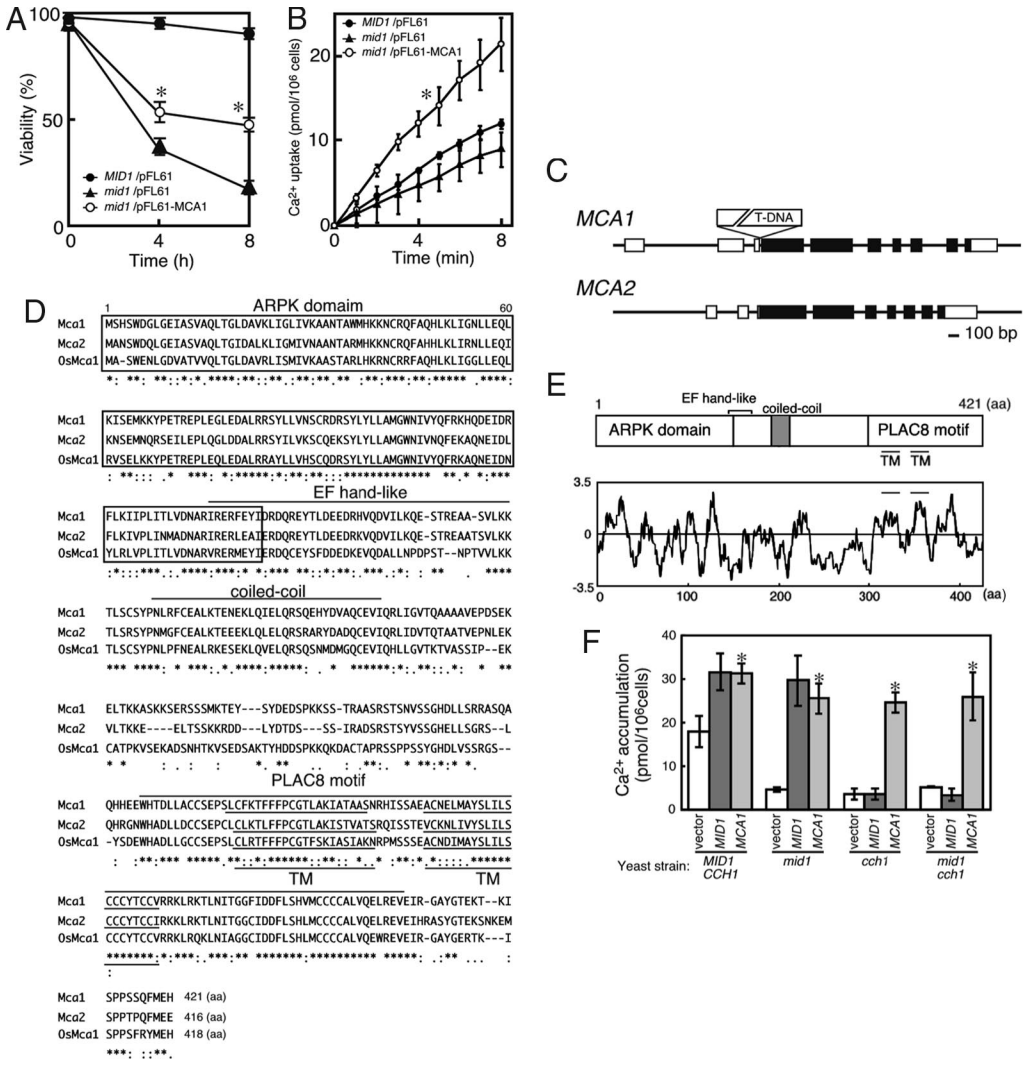

Fig. 1. Function in yeast cells and structural features of Mca1 and Mca2. (*A*) Complementation of lethality of the yeast *mid1* mutant by *MCA1*. Cell viability of the *mid1* mutant strain bearing pFL61-MCA1 or empty vector pFL61 and wild-type strain bearing pFL61 was determined after being exposed to the mating pheromone α-factor. Data are means ± SD from three independent experiments. *, $P < 0.01$ versus *mid1*/pFL61. (*B*) Ca^{2+} uptake activity. Exponentially growing cells of the above strains were suspended in Hepes/Tris buffer containing 74 kBq/ml $^{45}CaCl_2$ (74 MBq/nmol) and aliquots of the suspension were taken at 1-min intervals over 8 min and filtered through a Millipore filter (type HA; 0.45 μm). The radioactivity retained on the filters was counted. Data are means ± SD from three independent experiments. *, $P < 0.01$ versus *mid1*/pFL61. (*C*) Genomic organization of the *MCA1* and *MCA2* genes. Boxes represent exons and their black areas show the ORF. T-DNA (drawn to an arbitrary size) is inserted into the site 28 bp upstream of the fourth exon, producing an *mca1*-null allele. (*D*) Multiple amino acid sequence alignment of the Mca1, Mca2, and rice OsMca1 with Clustal W (version 1.8). Amino acid sequence identity (and similarity) between Mca1 and Mca2 is 72.7% (89.4%), that between Mca1 and OsMca1 is 65.0% (90.3%), and that between Mca2 and OsMca1 is 57.2% (86.4%). Asterisk indicates identical amino acid; colon indicates amino acid with strong similarity; dot indicates amino acid with weak similarity. The ARPK domain (for amino-terminal domain of rice putative protein kinases) is boxed. The line under each sequence shows a potential transmembrane segment (TM) predicted by TopPred (19). The lines above the Mca1 sequence represent an EF-hand-like structure, a coiled-coil region, and a C-terminal, cysteine-rich region similar to the PLAC8 motif found in plant and animal proteins of unknown function. (*E*) Schema of Mca1 and the hydropathy profile of Mca1. The bars indicate the position of the potential transmembrane segments (TM) described in *D*. (*F*) *MCA1* has the ability to increase Ca^{2+} accumulation even in the *mid1 cch1* double mutant. *MCA1* cDNA on a plasmid was expressed under the control of the *TDH3* promoter in each yeast mutant (*mid1*, *cch1*, or *mid1 cch1*) as well as the parental strain (*MID1 CCH1*). The *MID1* gene was expressed from the plasmid YEpMID1 (25). Exponentially growing cells were incubated for 2 h in the low Ca^{2+} medium SD.Ca100 (15) containing 185 kBq/ml $^{45}CaCl_2$ (1.8 kBq/nmol) and aliquots of the culture were taken and filtered through a Millipore filter (type HA; 0.45 μm). *, $P < 0.05$ versus vector in each mutant.

The *MCA1* gene (DDBJ accession no. AB196960) has 10 exons and was predicted to encode a polypeptide of 421 amino acid residues (Fig. 1 *C* and *D*). The overall amino acid sequence has only 10% identity and 41% similarity to that of the Mid1 protein and has no significant similarity to that of any protein characterized as an ion channel component. The TopPred (19), TMPred (20), and PredictProtein (21) programs suggested that Mca1 has at least two potential transmembrane segments (Fig. 1 *D* and *E*). The carboxyl-terminal half shows similarity to the PLAC8 (for human placenta-specific gene 8) region that is a cysteine-rich domain of unknown function found in 127 plant and animal proteins (22). The Mca1 amino-terminal half has an EF hand-like motif and is similar to a functionally unknown, amino-terminal domain found in many rice putative protein kinases [designated the ARPK domain for amino-terminal domain of rice putative protein kinases; see supporting information (SI) Fig. 5].

Previous studies have shown that Mid1 cooperates with Cch1, which is homologous to the α1 subunit of mammalian voltage-gated Ca^{2+} channels, to function as a putative Ca^{2+}-permeable

channel in yeast (23, 24). Thus, *MID1* even on a multicopy plasmid is unable to complement the Ca^{2+}-uptake defect of the *mid1 cch1* double mutant (ref. 25; Fig. 1*F*). By contrast, *MCA1* was able to do so (Fig. 1*F*). This Cch1-independent complementation by Mca1 suggests that Mca1 functions in a way different from Mid1.

A Blast search (BLASTP) (26) with the amino acid sequence of Mca1 showed 73% full-length identity to a hypothetical *Arabidopsis* ORF of unknown function (At2g17780) on chromosome 2. We designated its gene (DDBJ accession no. AB196961) *MCA2*. The features of the gene organization and protein structure are similar to those of Mca1 (Fig. 1 *C* and *D*), suggesting that the functions of these two proteins are similar. The Blast search (TBLASTN) (26) also identified a rice cDNA clone, J033126N07, which encodes an orthologue (designated OsMca1) of Mca1 with 65% full-length identity (Fig. 1*D*), suggesting that Mca1 constitutes a unique family in flowering plants.

Expression and Subcellular Localization of Mca1. *MCA1* mRNA was expressed in various organs of mature *Arabidopsis* examined, including roots, leaves, stems, flowers and siliques, with diverse expression levels (Fig. 2*A*). Fluorescence microscopy suggested that the Mca1-GFP fusion protein, produced under the control of the 35S promoter of the cauliflower mosaic virus (CaMV), was present in the plasma membrane of root cells (Fig. 2*B*), and this suggestion was strengthened by treatment with a high osmotic solution (0.8 M mannitol) that induced plasmolysis. The localization and behavior of Mca1-GFP were very similar to those of a plasma membrane marker protein (27) and different from those of marker proteins (27) for the endoplasmic reticulum and the vacuole as well as those of cytoplasmic GFP, all of which were also expressed under the control of the CaMV 35S promoter. We made anti-Mca1 antibodies that specifically recognize Mca1 expressed in yeast, but they did not detect Mca1 in *Arabidopsis* protein preparations by immunoblotting, probably because it is low in content or solubility. Therefore, we used yeast cells expressing Mca1 for examining its subcellular localization. Membrane fractionation experiments indicated that Mca1 is localized to the yeast plasma membrane as an integral membrane protein (Fig. 2 *C* and *D*). These results suggest that Mca1 is a plasma membrane protein responsible for Ca^{2+} influx in *Arabidopsis*.

Mca1 Promotes Ca^{2+} Influx upon Mechanical Stimulation *in Planta*. To determine the function of Mca1 *in planta*, we isolated an *mca1*-null mutant line from T-DNA insertion populations using PCR-based screening. In the null mutant, T-DNA was found to have inserted into a position 28 bp upstream of the fourth exon, corresponding to 28 bp upstream of the initiation codon, of the *MCA1* locus (Fig. 1*C*), leading to no production of *MCA1* mRNA, as revealed by RT-PCR (Fig. 3*A*). The *mca1*-null mutant grew like the wild type under ordinary growth conditions and on medium containing low or high $CaCl_2$ (data not shown). We also made *Arabidopsis* transgenic lines (designated *MCA1*ox) that overexpress *MCA1* cDNA under the control of the CaMV 35S promoter. Three independent, representative lines showed increased expression of *MCA1* mRNA, although the expression levels varied from line to line, as revealed by Northern blotting (Fig. 3*B*). The development of the *MCA1*ox lines was abnormal and dependent on the expression levels (see below).

Using the *mca1*-null mutant and *MCA1*ox lines as well as the wild type, we directly measured Ca^{2+} uptake in the intact roots of 5-week-old-plants using $^{45}Ca^{2+}$ and found that *MCA1*ox roots incorporated Ca^{2+} to a greater extent than wild-type and *mca1*-null roots (Fig. 3*C*). This incorporation was almost completely inhibited by Gd^{3+}, a blocker of nonselective cation channels, including SA channels, but not by verapamil, a blocker of voltage-gated Ca^{2+} channels.

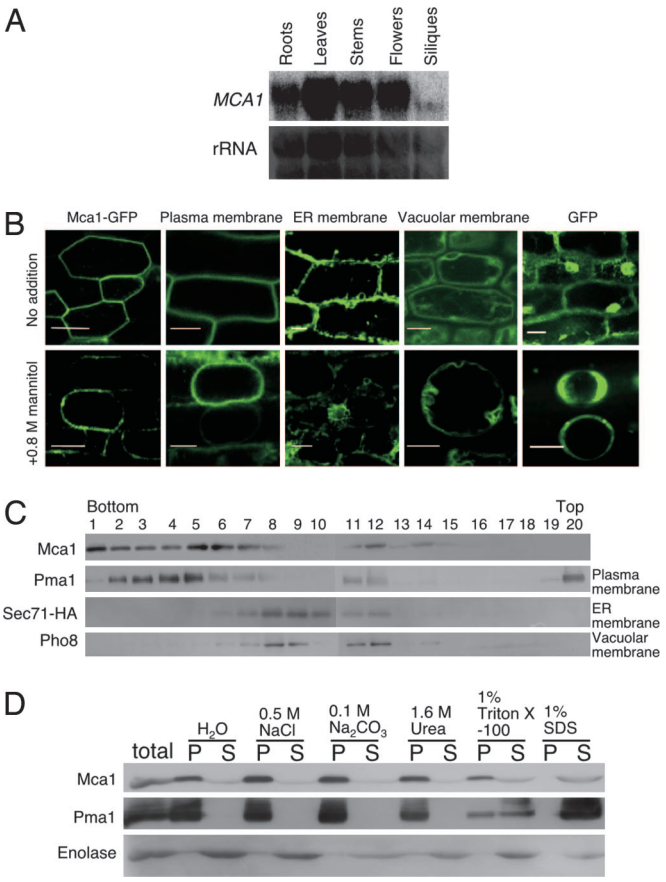

Fig. 2. Expression of *MCA1*. (*A*) Northern blotting of the *MCA1* transcripts. Total RNA was isolated from roots, leaves, stems, flowers, and siliques of mature *Arabidopsis* plants and subjected to Northern blotting. rRNA was used for internal controls for the amount of RNA loaded. (*B*) GFP fluorescence images suggesting the localization of Mca1-GFP in the plasma membrane of root cells. The upper row represents intact roots and the bottom row those treated with 0.8 M mannitol for at least 10 min. Note that mannitol induced plasmolysis. The sample and membrane marker proteins used are as follows: Mca1-GFP, a GFP fusion to the C terminus of the full length Mca1 protein; Plasma membrane, a GFP fusion to the plasma membrane channel protein PIP2A expressed in line Q8 (27); ER membrane, a GFP fusion to an endoplasmic reticulum membrane protein expressed in line Q4 (27); Vacuolar membrane, a GFP fusion to the vacuolar membrane channel protein delta-TIP expressed in line Q5 (27); and cytoplasmic GFP. (Scale bars, 20 μm.) (*C*) Membrane fractionation by sucrose density gradient centrifugation and localization of Mca1 expressed in yeast. Pma1, plasma membrane H^+-ATPase; Sec71-HA, an endoplasmic reticulum membrane protein tagged with hemagglutinin antigen (HA); Pho8, a vacuolar membrane protein. (*D*) Mca1 is an integral membrane protein in yeast. Note that Mca1 is not solubilized with NaCl, Na_2CO_3, and urea, all of which are known to solubilize peripheral membrane proteins. P, pellet after centrifugation at 100,000 $\times$ *g* for 1 h, containing membranes; S, supernatant.

To investigate the relationship between Mca1 and a mechanical stress-generated Ca^{2+} signal, seedlings of the wild-type, *mca1*-null, and *MCA1*ox lines having the Ca^{2+}-indicator protein aequorin were exposed to hypoosmotic stress (6) or the anionic amphipath trinitrophenol (TNP), which preferentially penetrates the outer leaflet of the plasma membrane (28). Both treatments generate membrane distortion, resulting in an activation of SA channels (6, 28). The results showed that the degree of $[Ca^{2+}]_{cyt}$ increase was markedly greater in the *MCA1*ox seedlings than in the wild-type ones and that there was no significant difference in $[Ca^{2+}]_{cyt}$ changes between the *mca1*-null and wild-type seedlings (Fig. 3 *D* and *E*). The hypoosmotic

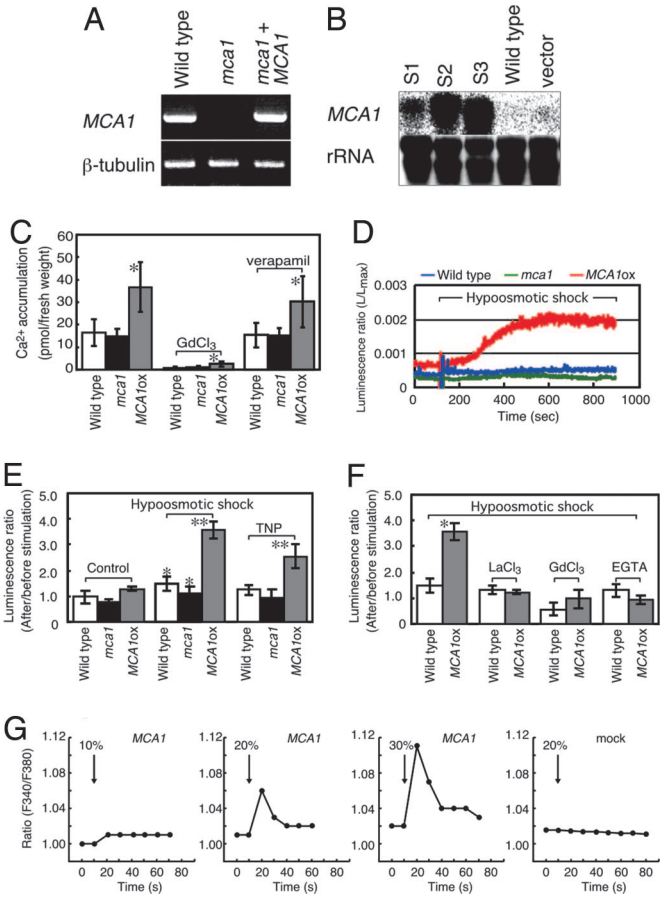

Fig. 3. Mca1 protein enhances Ca^{2+} uptake activity *in planta*. (*A*) RT-PCR showing no detectable production of *MCA1* transcripts in the *mca1*-null line. β-tubulin is a control. (*B*) Northern blotting, showing *MCA1* mRNA levels in *MCA1*ox (S1, S2, and S3), wild-type, and vector-bearing wild-type lines. rRNA was used for control experiments. (*C*) Overexpression of Mca1 increases Ca^{2+} uptake in intact roots. The roots were incubated with $^{45}CaCl_2$ for 20 min and washed five times with a washing solution containing $LaCl_3$, which displaces $^{45}Ca^{2+}$ nonspecifically bound to the cell wall (33). The uptake is inhibited by 1 mM Gd^{3+}, but not by 20 μM verapamil. *, $P < 0.01$ versus wild type. (*D*) Hypoosmotic shock-induced $[Ca^{2+}]_{cyt}$ changes, as revealed in aequorin luminescence. Wild-type, *mca1*-null, and *MCA1*ox seedlings with aequorin in MS medium (400 μl) were subjected to hypoosmotic shock with the addition of H_2O (200 μl). Representative data are shown for each seedling. (*E*) Summary of hypoosmotic shock- and TNP-induced $[Ca^{2+}]_{cyt}$ changes. As for hypoosmotic shock, experimental conditions were the same as those in *D*. For TNP stimulation and control experiments, 0.3 mM TNP (200 μl) and MS medium (200 μl) were added to the seedlings in MS medium (400 μl), respectively. The average of five independent experiments is shown for each sample. *, $P < 0.05$ versus each control; **, $P < 0.005$ versus wild type in each treatment. (*F*) Effect of channel blockers and a Ca^{2+} chelator on the hypoosmotic shock-induced $[Ca^{2+}]_{cyt}$ increase. Ten minutes before hypoosmotic shock, 1 mM La^{3+}, 1 mM Gd^{3+}, or 5 mM EGTA (calcium chelator) was added to the medium. *, $P < 0.005$ versus wild-type and reagent-treated samples. (*G*) Stretch-activated Ca^{2+} response in *MCA1*-expressing and mock-transfected CHO cells. Cells cultured on elastic silicone membranes were loaded with 1 μM fura-2/AM and subjected to a uniaxial stretch pulse (10, 20, or 30% of the length for 1 s at room temperature). Fura-2 fluorescence intensities at excitation wavelengths of 340 and 380 nm were acquired and the ratio (F340/F380) was calculated. An increase in the ratio donates a $[Ca^{2+}]_{cyt}$ increase. (*Right*) Mock-transfected cells. (*Center* and *Left*) *MCA1*-expressing cells.

stress-induced increase observed in the *MCA1*ox seedlings was inhibited by extracellulary applied La^{3+}, Gd^{3+}, or EGTA (Fig. 3*F*). These results suggest that Mca1 is involved in generating a Ca^{2+} signal upon plasma membrane distortion.

To examine this suggestion, we directly stretched *MCA1*-expressing mammalian cultured cells. *MCA1* cDNA was placed under the control of the Zn^{2+}-inducible human metallothionein IIa promoter in a plasmid and introduced into Chinese hamster ovary (CHO) cells as described (16, 29). The CHO cells were cultured on a fibronectin-coated silicone membrane, loaded with the Ca^{2+} indicator fura-2/AM, and subjected to uniaxial stretching for 1 s. As shown in Fig. 3*G*, although mock-transfected CHO cells treated with $ZnCl_2$ showed no increase in the fura-2 fluorescence ratio (F340/F380) that represents $[Ca^{2+}]_{cyt}$ ($n = 808$), *MCA1*-expressing CHO cells treated with $ZnCl_2$ showed an increase in the ratio, depending on the degree of stretching (40 of 765 cells; 5.2%), where the mean increase was 2.6% ± 0.34 SE ($n = 40$; $P < 0.01$, Fisher–Behrens t test).

Taken together, these cumulative data obtained with three different approaches suggest that Mca1 works in a Ca^{2+}-permeable SA channel system in the plasma membrane. The reason why there was no significant difference in the Ca^{2+} uptake and $[Ca^{2+}]_{cyt}$ increase between the wild-type and *mca1*-null lines remains uncertain at present; the activation of a compensatory mechanism in the null mutants may make the difference obscure.

Phenotypes of *MCA1*ox and *mca1*-Null Mutants. To characterize the physiological role of Mca1 *in vivo*, we investigated the phenotype of *MCA1*ox plants. Seedlings of one line (designated S3) expressing *MCA1* mRNA at a relatively high level (Fig. 3*B*) showed browning of the hypocotyls in ≈9 days (Fig. 4*A*), and most of them eventually died within ≈20 days after germination. Another line (S1) expressing *MCA1* mRNA at a relatively low level (Fig. 3*B*) developed milder symptoms than the S3 line, exhibiting developmental defects with short stems, small rosettes, no petals, shrunken siliques (Fig. 4*B*), and poor fertility (data not shown). Interestingly, leaf development was aggravated when the seedlings were grown on high-Ca^{2+} medium, but abrogated when they were grown on low (0.5 mM) Ca^{2+} medium (Fig. 4*C*). Essentially the same result was obtained with two other *MCA1*ox lines that are similar to the S1 line in *MCA1* mRNA levels (data not shown). This result is consistent with the above findings that Mca1 is responsible for Ca^{2+} influx.

To assess a physiological relevance of the overexpression of *MCA1*, we performed a quantitative RT-PCR analysis and found that *MCA1*ox plants had a constitutively elevated expression of a touch gene, *TCH3* (*CML12*), encoding a Ca^{2+}-binding, calmodulin-related protein whose expression is known to be induced by touch and Ca^{2+} (ref. 30 and SI Fig. 6), suggesting that Mca1 stimulates the expression and activity of Tch3 through Ca^{2+} influx.

Because the root, where *MCA1* mRNA is expressed, is a touch-sensitive organ that detects the hardness of soil during development (5), we examined whether the primary root of the *mca1*-null mutant failed to sense and adapt to the hardness of agar in medium. We thus developed a method, designated the two-phase-agar method, in which we used lower (harder) medium containing 1.6% agar covered with upper (softer) medium containing 0.8% agar, to observe root growth at the interface between the upper and lower media. Seeds were placed on the surface of the upper medium and allowed to develop into seedlings. It took both the primary roots of *mca1*-null and wild-type seedlings 5–7 days to reach the interface of the two-phase agar after sowing ($n = 150$ for each line). Although the primary root of the wild type was capable of penetrating the lower medium, that of a significant population of the *mca1*-null mutant was not (Fig. 4 *D* and *E*). Complementation of the *mca1*-null mutant with the extrinsic wild-type *MCA1* gene confirmed that *MCA1* is indeed responsible for this phenotype. Interestingly, when seeds were directly placed on 1.6% agar medium, the primary root of the *mca1*-null mutant was able to penetrate the medium, like that of the wild type. There was no

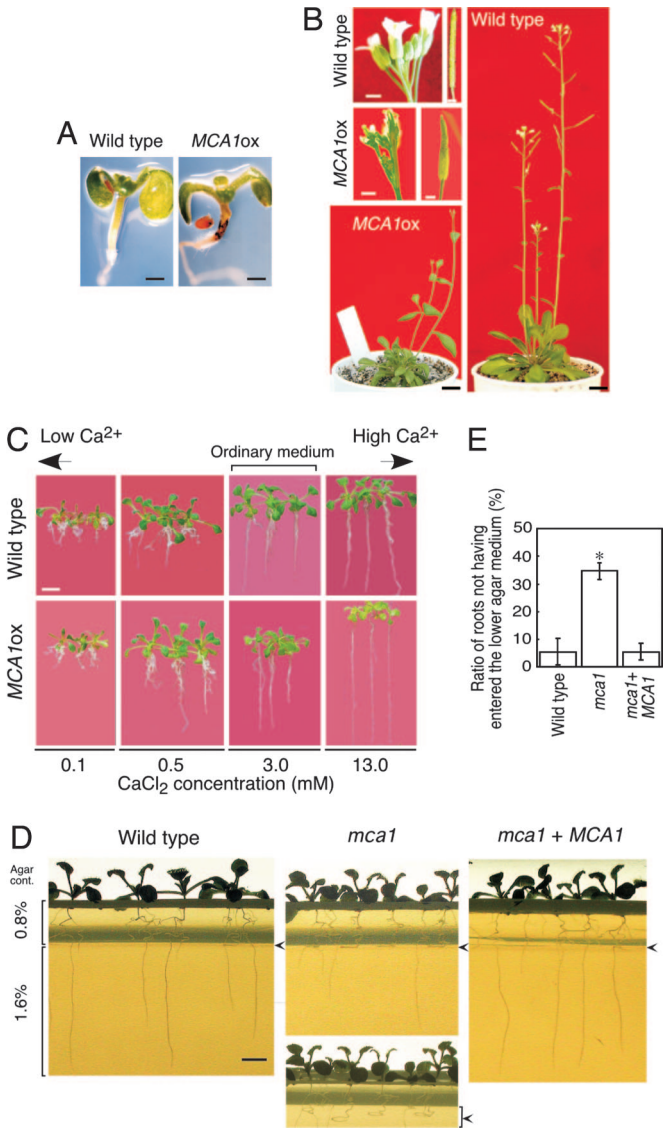

Fig. 4. Phenotypes of *mca1*-null and *MCA1*ox lines. (*A*) A seedling of the *MCA1*ox line S3, showing browning of the hypocotyl. (Scale bars, 2.0 mm.) (*B*) An *MCA1*ox plant (line S1), showing a phenotype with no petals, shrunken siliques, short stems, and small rosettes. (White bars, 1.5 mm; black bars, 1.0 cm.) (*C*) Ca^{2+}-dependent growth phenotypes of *MCA1*ox seedlings (line S1). Note that the ordinary MS medium contains 3.0 mM $CaCl_2$. On this medium, *MCA1*ox seedlings exhibited growth deficiency. (Scale bar, 1.0 cm.) (*D*) Failure to penetrate the lower, harder agar (1.6%) medium of the primary roots of the *mca1*-null mutant. Seeds of various lines were placed on the surface of the upper, softer agar (0.8%) medium of the two-phase-agar medium, allowed to grow for 9 days, and then photographed. (*Left*) Wild type (side view). (*Upper Center*) *mca1*-null (side view). (*Lower Center*) *mca1*-null (oblique upper view), showing the root tips were coiled at the interface of the two agar media. (*Right*) *mca1*-null mutant complemented with wild-type *MCA1*. Arrowheads represent the interface of the two agar media. (Scale bar, 1.0 cm.) (*E*) Quantitative representation of the results shown in *D*. Number of seedlings examined: Wild type, $n = 150$; *mca1*-null, $n = 150$; *mca1*-null + *MCA1*, $n = 80$. *, $P < 0.01$ versus wild type and *mca1*-null + *MCA1*.

difference in the length of the primary roots between the *mca1*-null and wild-type lines when they were grown in both 0.8 and 1.6% agar media ($n > 65$ primary roots for each medium).

Discussion

***Arabidopsis* Mca1 Mediates Ca^{2+} Uptake in Yeast.** The present study provides supporting evidence that Mca1 is a component of a plasma membrane Ca^{2+} influx system. Using a yeast screening system, we have cloned *Arabidopsis MCA1* cDNA that complements both the lethality and low Ca^{2+} uptake activity of the yeast *mid1* mutant defective in a putative Ca^{2+}-permeable SA channel component. Ca^{2+} incorporation assays, computer analysis of the predicted amino acid sequence, and membrane fractionation experiments have demonstrated that Mca1 is localized to the yeast plasma membrane as an integral membrane protein that mediates Ca^{2+} uptake.

From structural and mechanistic viewpoints, however, Mca1 is very different from Mid1, although *MCA1* complements the *mid1* mutant. An amino acid sequence alignment suggests that Mca1 is not an orthologue of Mid1. Because Mid1 cooperates with Cch1 to function as a Ca^{2+} influx system, Mid1 is unable to complement the low Ca^{2+} uptake activity of the *mid1 cch1* double mutant (25). By contrast, Mca1 can complement not only the *mid1* mutant, but also the double mutant. This ability is particularly interesting, because the yeast *S. cerevisiae* has only one high-affinity Ca^{2+} influx system, which is composed of Mid1 and Cch1 and becomes functional when cells are incubated in the low-Ca^{2+} medium that we have used in this study (31). Thus, it is remarkable that Mca1 can mediate Ca^{2+} uptake in yeast cells lacking the high-affinity Ca^{2+} influx system. This evidence supports a hypothesis that Mca1 is a Ca^{2+}-permeable transport protein. An alternative possibility that Mca1 activates another yeast endogenous transport system, however, cannot be completely ruled out.

Structural Features of Mca1. Mca1 has no overall sequence similarity to all known ion channels. However, there are several structural features of interest, the importance of which should be addressed experimentally in further studies: First, Mca1 has at least two transmembrane segments. This finding is consistent with membrane fractionation experiments with yeast cells, showing that Mca1 is an integral membrane protein; Second, the amino-terminal region is similar in amino acid sequence to that of rice putative protein kinases whose carboxyl-terminal region is predicted to have a catalytic function, suggesting that the amino-terminal region has a regulatory role; Third, the amino-terminal half has an EF-hand-like sequence, suggesting that the function of Mca1 is regulated by Ca^{2+}. Finally, the carboxyl-terminal half contains a region similar to the cysteine-rich PLAC8 domain of unknown function found in many plant and animal proteins (22).

Mca1 May Mediate Mechanically Stimulated Ca^{2+} Uptake in *Arabidopsis*. Mca1 appears to be involved in Ca^{2+} uptake across the plasma membrane in response to mechanical stimulation in *Arabidopsis*. First, fluorescence microscopy has suggested that the Mca1-GFP fusion protein is localized to the plasma membrane, and this suggestion is reinforced by the aforementioned membrane fractionation experiments with yeast cells expressing Mca1. Second, the roots of *MCA1*ox plants accumulate $^{45}Ca^{2+}$ more than those of wild-type and *mca1*-null plants. This accumulation is blocked by Gd^{3+}, which is known to inhibit SA channels. Third, *MCA1*ox plants also show increasing $[Ca^{2+}]_{cyt}$ in response to mild hypoosmotic shock and the amphipathic membrane crenator TNP, whereas wild-type and *mca1*-null plants do not. The $[Ca^{2+}]_{cyt}$ increase is blocked by Gd^{3+}, La^{3+}, and EGTA added to the medium. Fourth, *MCA1*-expressing CHO cells show an increase in $[Ca^{2+}]_{cyt}$ in response to cell stretching. In addition, our preliminary experiments with whole-cell patch-clamp recordings on mesophyll protoplasts have demonstrated that TNP-induced Ca^{2+} currents are statistically greater ($P < 0.01$) in *MCA1*ox protoplasts (2.3 ± 0.5 pA/pF at -80 mV; $n = 5$) than the wild-type and *mca1*-null protoplasts (0.5 ± 0.2 and 0.3 ± 0.2 pA/pF at -80 mV, respectively; $n = 5$ for each). These results suggest that Mca1 has a role in Ca^{2+} uptake in response to

membrane distortion in *Arabidopsis*. It should be noted that this suggestion relies on the overexpression of *MCA1*, which may cause side effects. In addition, we have observed no significant difference in the foregoing phenotypes between wild-type and *mca1*-null plants. Thus, more decisive experiments are needed to verify this suggestion.

Physiological Relevance and Working Model. Previous physiological studies have indicated that touch sensitivity is mediated by Ca^{2+} in the root tip. In the maize primary root, the root grows away from an agar block when the block is unilaterally applied to the root cap as a touch stimulus, and this response is enhanced when the agar contains Ca^{2+} (32). In the *Arabidopsis* primary root, touch induces a transient increase in $[Ca^{2+}]_{cyt}$ in all regions of the root, including the cap and the meristematic, elongation, and differentiated zones (5). The *Arabidopsis* root plasma membrane has been electrophysiologically shown to have nonselective cation channels that mediate Ca^{2+} uptake (33). However, proteins or genes critically involved in these processes have remained to be uncovered.

We have found that the primary roots of the *mca1*-null seedlings are incapable of penetrating a lower (harder) agar surface (1.6%) after growth through an upper (softer) agar (0.8%) medium. Because only one T-DNA insertion allele is available, we have confirmed this finding by complementation with a wild-type copy of the *MCA1* gene. It is unlikely that the primary roots of *mca1*-null seedlings merely grow weakly, because when the *mca1*-null seeds are directly sowed on 1.6% agar medium, the primary roots can penetrate it, like the wild-type primary roots. In addition, the primary roots of *mca1*-null and wild-type seedlings simultaneously reaches the interface of the upper and lower agar media in 5–7 days from the surface of the upper medium, and the length of the primary roots is essentially the same between the two seedlings, as described in *Results*, suggesting that the *mca1*-null mutation does not affect the growth rate of the primary root. Therefore, we suggest that Mca1 is required for sensing the hardness of agar or soil. Furthermore, these results suggest that conditioning or hardening of the primary roots for mechanosensing and response may be established in an early stage after germination.

Taken together, we propose a working model that Mca1 is crucial for mechano-stimulated Ca^{2+} uptake and mechanosensing in the primary root. Because the calmodulin-like protein Tch3 or Cml12, a cytosolic Ca^{2+}-signaling protein known to be induced by touch and Ca^{2+} in many tissues of *Arabidopsis*, including roots (30), is overproduced in *MCA1*ox plants, Mca1 could have a physiologically relevant role in these processes. Further study on Mca1 and its family, such as Mca2 and OsMca1, should facilitate exploration of how plants expand their roots in highly complex but well organized ways.

Materials and Methods

Plant Growth Conditions. The Columbia-0 (Col-0) ecotype of *A. thaliana* and its isogenic, transgenic lines were used. Seeds were sterilized with 70% ethanol for 10 s and then with 1% Antiformin for 10 min, and sown on MS/1% sucrose agar medium. MS medium contained Murashige and Skoog salts (34), 1× Gamborg's vitamin solution (Sigma Aldrich, Taufkichen, Germany), and 2.56 mM Mes-KOH, pH 5.7. Calcium-free Murashige and Skoog salts were made according to the formula of Murashige and Skoog (34) with the removal of $CaCl_2$. For low-calcium medium, agarose was used instead of agar. Plants were grown at 22°C under 16-h light conditions at 40–60 μM m^{-2} s^{-1} light intensity.

Supporting Information. For other methods, see *SI Text*.

We thank Dr. M. Minet (Centre de Génétique Moléculaire, Centre National de la Recherche Scientifique, Gif sur Yvette, France) for the *A. thaliana* cDNA library; Dr. K. Kuchitsu for valuable discussion; Dr. A. Sugino (Osaka University, Osaka, Japan) for plasmids; Dr. Y. Ohsumi (National Institute for Basic Biology, Okazaki, Japan) for anti-Pho8 antibodies; Ms. Y. Moriya for technical assistance; and Ms. Y. Higashi for secretarial assistance. This work was supported by Grants-in-Aid from the Japanese Ministry of Education, Culture, Sports, Science and Technology and CREST and ICORP/SORST, Japan Science and Technology Agency.

1. Darwin C (1880) *The Power of Movement in Plants* (John Murray, London).
2. Trewavas A, Knight M (1994) *Plant Mol Biol* 26:1329–1341.
3. Braam J (2005) *New Phytol* 165:373–389.
4. Knight MR, Campbell AK, Smith SM, Trewavas AJ (1991) *Nature* 352:524–526.
5. Legué V, Blancaflor E, Wymer C, Perbal G, Fantin D, Gilroy S (1997) *Plant Physiol* 114:789–800.
6. Takahashi K, Isobe M, Knight MR, Trewavas AJ, Muto S (1997) *Plant Physiol* 111:587–594.
7. Cosgrove DJ, Hedrich R (1991) *Planta* 186:143–153.
8. Pickard BG, Ding JP (1993) *Aust J Plant Physiol* 20:439–459.
9. Taylor LP, Hepler PK (1997) *Annu Rev Plant Physiol Plant Mol Biol* 48:461–491.
10. Haswell ES, Meyerowitz EM (2006) *Curr Biol* 16:1–11.
11. Anderson JA, Huprikar SS, Kochian LV, Lucas WJ, Gaber RF (1992) *Proc Natl Acad Sci USA* 89:3736–3740.
12. Sentenac H, Bonneaud N, Minet M, Lacroute F, Salmon J-M, Gaymard F, Grignon C (1992) *Science* 256:663–665.
13. Ali R, Zielinski RE, Berkowitz GA (2006) *J Exp Bot* 57:125–138.
14. Gobert A, Park G, Amtmann A, Sanders D, Maathuis, FJ (2006) *J Exp Bot* 57:791–800.
15. Iida H, Nakamura H, Ono T, Okumura MS, Anraku Y (1994) *Mol Cell Biol* 14:8529–8271.
16. Kanzaki M, Nagasawa M, Kojima I, Sato C, Naruse K, Sokabe M, Iida H (1999) *Science* 285:882–886.
17. Kanzaki M, Nagasawa M, Kojima I, Sato C, Naruse K, Sokabe M, Iida H (2000) *Science* 288:1347.
18. Minet M, Dufour M-E, Lacroute F (1992) *Plant J* 2:417–422.
19. Hofmann K, Stoffel W (1993) *Biol Chem Hoppe-Seyler* 374:166.
20. Claros MG, von Heijne G (1994) *CABIOS* 10:685–686.
21. Rost B, Yachdav G, Liu J (2003) *Nucleic Acids Res* 32:W321–W326.
22. Marchler-Bauer A, Anderson JB, Cherukuri PF, DeWeese-Scott C, Geer LY, Gwadz M, He S, Hurwitz DI, Jackson JD, Ke Z, *et al.* (2005) *Nucleic Acids Res* 33:D192–D196.
23. Fischer M, Schnell N, Chattaway J, Davies P, Dixon G, Sanders D (1997) *FEBS Lett* 419:259–262.
24. Paidhungat M, Garrett S (1997) *Mol Cell Biol* 17:6339–6347.
25. Iida K, Tada T, Iida H (2004) *FEBS Lett* 576:291–296.
26. Altschul SF, Madden TL, Schäffer AA, Zhang J, Zhang Z, Miller W, Lipman DJ (1997) *Nucleic Acids Res* 25:3389–3402.
27. Cutler SR, Ehrhardt DW, Griffitts JS, Somerville CR (2000) *Proc Natl Acad Sci USA* 97:3718–3723.
28. Martinac B, Adler J, Kung C (1990) *Nature* 348:261–263.
29. Naruse K, Yamada T, Sokabe M (1998) *Am J Physiol* 274:H1532–H1538.
30. Braam J (1992) *Proc Natl Acad Sci USA* 89:3213–3216.
31. Muller EM, Locke EG, Cunningham KW (2001) *Genetics* 159:1527–1538.
32. Ishikawa H, Evans ML (1992) *Plant Physiol* 100:762–768.
33. Demidchik V, Bowen HC, Maathuis FJM, Shabala SN, Tester MA, White PJ, Davies JM (2002) *Plant J* 32:799–808.
34. Murashige T, Skoog S (1962) *Physiol Plant* 15:473–497.